Cement and Concrete Research 40 (2010) 885–891

Contents lists available at ScienceDirect

Cement and Concrete Research

journal homepage: http://ees.elsevier.com/CEMCON/default.asp

Micro-spectroscopic investigation of Al and S speciation in hardened cement paste

E. Wieland [a,*], R. Dähn [a], M. Vespa [b], B. Lothenbach [c]

[a] Laboratory for Waste Management, Nuclear Energy and Safety Research Department, Paul Scherrer Institute, 5232 Villigen PSI, Switzerland
[b] Flemish Organization of Scientific Research (FWO), Dutch-Belgium Beamline (DUBBLE), BP-220, 38043 Grenoble Cedex 9, France
[c] Laboratory for Concrete and Construction Chemistry, Swiss Laboratories for Materials Testing and Research (Empa), 8600 Dübendorf, Switzerland

ARTICLE INFO

Article history:
Received 17 August 2009
Accepted 1 February 2010

Keywords:
Hydration products (B)
Spectroscopy (B)
Cement paste (D)
Monosulfate (D)
Ettringite (D)

ABSTRACT

Synchrotron-based micro X-ray fluorescence (micro-XRF) and micro X-ray absorption near edge spectroscopy (micro-XANES) have been used to determine the spatial distribution of Al and S and to identify the Al- and S-bearing species in compact hardened cement paste hydrated at 50 °C. The contribution of the S-bearing cement phases to the composed S K-edge XANES spectra collected in ten S-rich regions was determined using least-squares fitting. Ettringite and calcium monosulfoaluminate were identified as the main S-bearing species in the selected regions. Factor analysis was employed to determine the contribution of the various Al-bearing cement minerals to the composed Al K-edge XANES collected in different Al-rich regions of the cement matrix. Principal component analysis revealed that all spectra could be fitted using three components. Target transformation further suggested that the two Al-bearing clinker phases (aluminate, ferrite) and secondary phases of the hydrate assemblage (ettringite, AFm phases, hydrotalcite) contributed to the set of components that made up the experimental spectra. Least-squares fitting allowed the relative contribution of each reference compound to be determined. Aluminate and/or ferrite were detected in all Al-rich regions. AFm phases were identified in six out of the ten regions studied, while ettringite was detected in only two regions. The study confirmed that AFm phases are important cement minerals in hardened cement paste hydrated at 50 °C.

1. Introduction

Hardened cement paste (HCP) comprises a very heterogeneous mineral assemblage with discrete cement minerals in the nano- to micrometer size range. The current understanding of the structure and chemical properties of this complex material has been achieved mainly using well-established techniques, such as X-ray diffraction (XRD), thermogravimetric analysis/differential thermogravimetry (TGA/DTA), and solid-state nuclear magnetic resonance [e.g., 1]. These techniques are of limited use if spatially resolved information on different mineral phases present in the compact material is required. Spatial information is particularly important with a view to improving our understanding of the chemical reactions taking place in highly reactive zones around clinker minerals. Scanning electron and transmission electron microscopy coupled with microanalysis (SEM/EDS, TEM/EDS) has been used to provide spatially resolved information on the microstructure coupled with the determination of the chemical composition of the local area [e.g. 2–4]. For example, SEM/EDS allowed the formation of distinct rims of inner C–S–H to be discerned based on grey level contrasts and the chemical composition of the rims to be determined using microanalysis [2]. In cementitious materials X-rays generated due to interaction of the incident electrons with matter typically probe an area of around 1–2 μm, which is larger than the size of hydrate phases [3]. This further implies that the chemical composition corresponds to mixture of phases rather than single phases.

Synchrotron-based micro X-ray absorption spectroscopy has proven a versatile tool to determine the coordination environment of impurity elements accumulated in the reactive zones around alite in simulated cement-stabilized waste forms [e.g., 5–7]. Micro-spectroscopic techniques can yield spatially resolved structural data, which may disclose the chemical speciation and processes at the molecular scale. Thus, the structural information obtained from analytical synchrotron-based X-ray probes is complementary to knowledge of the chemical composition and the microstructure in a local area of interest as obtained from SEM/EDS. The optics of modern X-ray analytical facilities allows micro-focusing studies to be performed with a spatial resolution of between 1 μm and 10 μm. Thus, the resolution is comparable to that achieved by SEM. In this study micro X-ray absorption near edge spectroscopy (micro-XANES) was utilized with the aim of evaluating the applicability of the technique for speciation studies in cement. The position of an absorption edge (or ionization energy of an atom) is unique to the type of atom that adsorbs X-rays. The redox state of an element may give rise to small shifts in the position. The region within about 30 eV from the edge position is referred to as the XANES range, which is often dominated by strong scattering processes of the excited electrons as well as local atomic resonances in X-ray absorption. Thus, XANES spectra contain specific

* Corresponding author. Tel.: +41 56 310 2291; fax: +41 56 310 3565.
E-mail address: erich.wieland@psi.ch (E. Wieland).

0008-8846/$ – see front matter © 2010 Elsevier Ltd. All rights reserved.
doi:10.1016/j.cemconres.2010.02.001

information on the local atomic structure of the absorber atom. Interpretation of XANES spectra, however, is presently limited to relatively qualitative level and often requires comparison with those of reference materials. The theory of XANES as well as potentials and limitations of the application of XANES in cementitious materials have been discussed in detail elsewhere [e.g., 7,8].

Over the past years synchrotron-based X-ray absorption spectroscopy (XAS) has been utilized to examine structural changes of hydrating calcium aluminates [e.g., 9–11] and to identify the coordination environment of Ca in calcium silicate hydrates [e.g., 12,13]. To the best of our knowledge, only few studies have used XAS techniques to determine the speciation of cement-derived elements such as Ca, Si and S in complex cementitious materials [14–16]. Verstraete et al. [14] investigated time-dependent changes in the coordination environment of Si during the alkali-activated reaction of aggregate materials. Pattanaik et al. [15] carried out Ca and S K-edge XAS investigations on crushed cementitious materials, which were produced using coal combustion by-products. S K-edge XANES allowed distinction of different oxidation states of sulfur in these cementitious materials, while Ca K-edge XANES further provided information on the kind of cement minerals formed in the matrix.

Previous studies on Portland cements indicated that in samples hydrated at 50 °C or above calcium monosulfoaluminate should form at the expense of ettringite [17,18]. Presence of calcium monosulfoaluminate was indicated from TGA/DTA and XRD [17]. Thermodynamic modelling further suggested that at 20 °C, calcium monocarboaluminate and ettringite are stable, while at 50 °C calcium monosulfoaluminate is more stable [18,19]. As a consequence, it was predicted that the amount of ettringite is significantly reduced at 50 °C. However, due to the low molar Al_2O_3/SO_3 (bulk weight) ratio of <1.3 of the sulfate resistant Portland cement (SRPC) cement used in the present study [19]. It was further predicted that small amounts of ettringite should persist in the SRPC paste. Furthermore, conversion of calcium monocarboaluminate to calcium monosulfoaluminate was expected to significantly decrease the amount of the former phase in HCP.

In the present study it was investigated whether or not ettringite and monosulfoaluminate co-existed locally in the same area of the cement matrix. Al and S K-edge XANES have been used to identify the Al- and S-bearing cement minerals present in selected regions of interest (ROI) of intact HCP with micro-scale resolution. Identification of these minerals was achieved by applying principal component analysis (PCA) and linear combination (LC) fitting as the resulting XANES were considered to be composed spectra containing contributions from different species of the absorber atom. Thus, analysis of the data was based on the notion that the local structure of Al and S in the Al- and S-bearing cement minerals causes characteristic contributions to the composed XANES spectra. This assumption was supported by earlier XANES studies on S-bearing cement minerals [7,15,16], while, for example, the study of Doyle et al. [20] showed that the Al K-edge XANES spectra of Al-bearing natural minerals are distinctly different. Al and S speciation was studied using intact HCP prepared from SRPC for which the hydration process was previously investigated as a function of time and temperature [17–19].

2. Experimental

2.1. Sample preparation

2.1.1. Materials

Throughout this study Sigma-Aldrich or Merck “pro analysis” chemicals and a high-purity de-ionised water (18.2 MΩ cm) generated by a Milli-Q Gradient A10 System (Millipore) were used for the preparation of the solutions. Handling of materials (e.g. sampling etc.) was carried out in a glovebox under a controlled N_2 atmosphere (O_2 and $CO_2 \leq 2$ ppm) to avoid CO_2 contamination.

2.1.2. S-bearing reference compounds

Ettringite ($Ca_6Al_2(SO_4)_3(OH)_{12}\cdot 26H_2O$) was prepared according to a procedure reported elsewhere [21]. Calcium monosulfoaluminate ($Ca_4Al_2(SO_4)(OH)_{12}\cdot 6H_2O$) was synthesized by Matschei et al.[22]. Calcium sulfate-dihydrate ($CaSO_4\cdot 2H_2O$) was purchased from Sigma-Aldrich (Buchs, Switzerland).

2.1.3. Al-bearing reference compounds

Pure tricalcium aluminate (C_3A ($Ca_3Al_2O_6$), cubic) was prepared from a 3:1 molar ratio of $CaCO_3$ and Al_2O_3. The starting materials were mixed in an agate mortar using few water droplets to prepare a homogenous paste. The mixture was placed in a platinum crucible and heated at 800 °C for 1 h and after that, 4 h at 1000 °C to eliminate adsorbed water and CO_2. The material was ground before and after each ignition step (12 h at 1450 °C), which was repeated several times. Brownmillerite, C_4AF ($Ca_4Al_2Fe_2O_{10}$) was purchased from Mineral Research Processing (Meyzieu, France). The AFm phases calcium monocarboaluminate, ($Ca_4Al_2(CO_3)(OH)_{12}\cdot 5H_2O$), and hydroxy-AFm (tetra-calcium aluminate hydrate C_4AH_{13}; $Ca_4Al_2(OH)_{14}\cdot 6H_2O$) were prepared by Matschei et al. [22]. Further, synthesis of Si-hydrogarnet ($Ca_3Al_2(SiO_4)_{0.8}(OH)_{8.8}$) and CO_3-hydrotalcite ($Mg_4Al_2(OH)_{12}\cdot CO_3\cdot 2H_2O$) used in this study were carried out by Matschei [23] and Rozov et al. [24].

2.1.4. Preparation of the HCP sample

The HCP sample was prepared from commercial SRPC CEM I 52.5 N HTS (Lafarge, France). Hydration and curing of the paste at 50 °C was described elsewhere [17]. After curing for 28 days the cement paste was immersed in acetone for 24 h to stop the hydration process and dried in the vacuum oven at 40 °C. The thin section was prepared by polishing the HCP material after pressure impregnation with epoxy resin (Th. Beckmann, Soil morphology, Schwülper-Lagersbüttel, Germany, pers. comm.). Silver spots were applied on the thin sections and used as markers to localize regions of interest.

2.2. Micro-XRF/XAS data collection

Micro-XRF mapping of the Al, Si, Mg and S distribution was performed at the Swiss Light Source (SLS), Switzerland, on the LUCIA beamline [25]. The micro-XRF maps were obtained by scanning the sample in vacuum (10^{-3} mbar) under the monochromatic beam at 3900 eV (below the Ca K-edge) and a beam size of about $3\times 3\ \mu m^2$. The emitted fluorescence X-rays were detected with a single-element silicon drift diode detector.

The Al K-edge (1559.6 eV) XANES measurements were carried out using the YB66 (yttrium 66 boride) crystal, while the S K-edge (2472 eV) measurements were conducted using the Si(111) monochromator. The monochromator angle was calibrated by assigning the energy of 1559.6 eV to the first inflection point of the K-edge absorption spectrum of Al metal foil and to 2472 eV to the first inflection point of the K-edge absorption spectrum of crystalline sulfur. All XANES spectra were recorded in fluorescence-yield mode using the single-element drift diode detector. The lateral size, the penetration depth of the X-ray beam, and the escape depths of X-ray fluorescence determined the volume probed for each micro-XANES spectrum. The depth of X-ray penetration was slightly less near the Al K-edge (~3.6 μm at 1559.6 eV) than the S K-edge (~9.4 μm at 2472 eV) [7]. The escape depths were similar to the penetration depths for both Al and S Kα fluorescence, indicating that volumes of a few tens of μm^2 were probed, possibly containing several species. Note that the typical crystal sizes of cement minerals range from a few nanometers (hydrate phases) to several hundreds of micrometers (clinker minerals). Identification of the species contributing to the composed micro-XANES spectra required comparison with the XANES spectra of reference compounds. The reference samples were prepared by grinding 50 mg of the reference compound in an agate mortar. The powder samples were pressed into pellets, which were

mounted on copper slides using adhesive tape. The Al and S K-edge XANES measurements on the reference compounds were carried out in the energy range from about 30 eV below the absorption edge up to about 170 eV above the absorption edge. The XANES spectra are shown for an energy range up to 30 eV above the absorption edge, which covers all main features detected in the XANES.

The micro-XRF maps were processed using the Labview software package available from beamline 10.3.2 of the Advanced Light Source (ALS) [26] and MATLAB. XANES data reduction was performed with the IFEFFIT software package (ATHENA) following standard procedures [27,28]. Pre-edge background subtraction and normalization were carried by fitting a first-degree polynomial to the pre-edge and a third-degree polynomial to the post-edge regions of the adsorption spectra [27,28]. The Al and S K-edge XANES spectra of the reference samples were corrected for self-absorption (Tröger et al. [29]) as implemented in ATHENA.

2.3. Data analysis and fitting

The normalized XANES spectra collected for selected ROIs of the cement matrix were analyzed following a two-step procedure similar to that proposed by Ressler et al. [30]: i) determination of the number of constituent species contributing to the XANES spectra and identification of suitable species from the available reference compounds using PCA and target transformation (TT), ii) quantification of the identified species in each ROI using the least-squares minimization.

Principal components analysis was carried out using the Labview software package of beamline 10.3.2 [26]. The program implements PCA as described by Ressler et al. [30]. The PCA procedure is based on the singular-value decomposition algorithm in linear algebra [e.g. 31], which allows the rectangular $M\times N$ matrix (A) to be presented as the product of the column-orthogonal $M\times N$ matrix (E), the diagonal $N\times N$ matrix (λ) with positive or zero elements and the transpose of an orthogonal $N\times N$ matrix (W) [30,32]:

$$A = E \times \lambda \times W \tag{1}$$

A is the set of spectra, which is factored into its components. Each column vector in A, thus, represents an experimental XANES spectrum of an unknown mixture (total N spectra) with M data points. The matrix E corresponds to the set of components into which A is decomposed, thus referring to the "eigenvectors". The matrix λ contains the scale factors according to the relative importance of each component, referring to the singular values or "eigenvalues", respectively. The dimension of the latter matrix indicates how many "eigenvalues" are sufficient to reproduce the experimental XANES spectra, thus representing the number of principal components present in the experimental data set. The matrix W is a table of weights showing the relative amount of a given component in each spectrum. Principal component analysis decomposes the spectra into "abstract" components, which do not resemble the spectra of "real" reference compounds. An additional criterion (IND) was introduced to determine the minimal number of reference compounds required [32]. According to this semi-empirical approach the last useful component is the one at which the factor IND is at its minimum.

Target transformation is the tool commonly used to test which reference compounds are necessary to reconstruct the experimental spectra [30,32]. The so-called SPOIL number was proposed as measure of the match between an abstract component and the real reference compound [30,32]. This number is <1.5 if the match is considered to be excellent. A value between 1.5 and 3 indicates good, 3 and 4.5 fair and 4.5 and 6 poor agreement, while >6 is considered to be an unacceptable match [32].

In this study PCA was applied to gain information on the number and type of constituent (reference) species in the ROIs analyzed in the cement matrix. Based on this information the least-square linear combination (LC) fitting as implemented in the IFEFFIT software package (ATHENA) was carried out to determine the contribution of the XANES spectrum of a reference compound to the experimental XANES spectra of the unknown mixture. The goodness of fit indicator, the R-factor, is defined as:

$$R = \frac{\sum_{i=1}^{m}\left(\mu_{i,\mathrm{exp}}-\mu_{i,\mathrm{fit}}\right)^2}{\sum_{i=1}^{m}\left(\mu_{i,\mathrm{exp}}\right)^2} \tag{2}$$

with $\mu_{\mathrm{i,exp}}$ as the normalized adsorption of the unknown sample and $\mu_{\mathrm{i,fit}}$ as the simulated adsorption based on the varying amounts of normalized XANES spectra of the reference compounds. The quality of fits is good if $R<0.02$.

3. Results and discussion

3.1. XRF mapping

Micro-XRF elemental maps were recorded in the first phase of this study in order to determine the distribution of cement-derived elements of interest i.e. Al, Si, S and Mg. The maps shown in Figs. 1 and 2 were recorded in two different areas of the intact HCP sample. In a previous study it was shown that micro-XRF maps and SEM generate slightly different images of the cement structure due to differences in resolution and the penetration depth of the electron and X-ray beam, respectively [7]. Figs. 1 and 2 show that the main features of the cement matrix were reproduced by the XRF maps, in particular the "patchy" distribution of the clinker minerals in the cement matrix as revealed from the Si maps.

Speciation studies were subsequently carried out at target spots for which the two different areas of the intact HCP sample were selected. The Al and S maps were used to localize those ROIs in the intact cement matrix where Al and S were enriched. Regions of high Al and high S concentrations could be distinguished from those with high Al concentrations but with low or no S contents. In the latter case the presence of non-hydrated and/or hydrated aluminates, respectively, such as calcium monocarboaluminate, was expected, while areas with high Al and S concentrations suggested presence of ettringite and/or calcium monosulfoaluminate. A total of ten ROIs (1–10) were selected in each area of the intact HCP sample based on visual inspection of the Al and S XRF maps for the Al and S K-edge micro-XANES measurements. Most ROIs were localized in reactive zones around clinker minerals. The counting statistics at all spots was checked to achieve a good signal to noise ratio. For the Al K-edge XANES measurements the ROIs were selected using the Al and Si XRF maps as a guide. The areas of interest were chosen in regions of high and medium Al contents to achieve the required counting statistics for the micro-XANES measurements. The areas contained non-hydrated aluminates (C_3A, C_4AF) and adjacent reactive zones around these clinker minerals (Fig. 2). Number and location of the ROIs were selected with a view to testing whether or not micro-XANES can be used to identify Al- and S-bearing cement minerals present in HCP.

3.2. XANES spectra of reference compounds

The energy positions and intensities of the absorption edges (white line) of all S reference compounds were similar, indicating presence of sulfur in oxidation state + VI [e.g., 33–35]. The white line can be attributed to the transition of the 1 s core electron to the lowest unoccupied antibonding states of the S atom. Distinct differences in the post-edge features were observed in the energy range between 2490 eV and 2510 eV (Fig. 3), which are due to multiple scattering resonances from neighboring atomic shells. The S K-edge XANES of calcium sulfate showed three features, 'A', 'B' and 'C', which did not

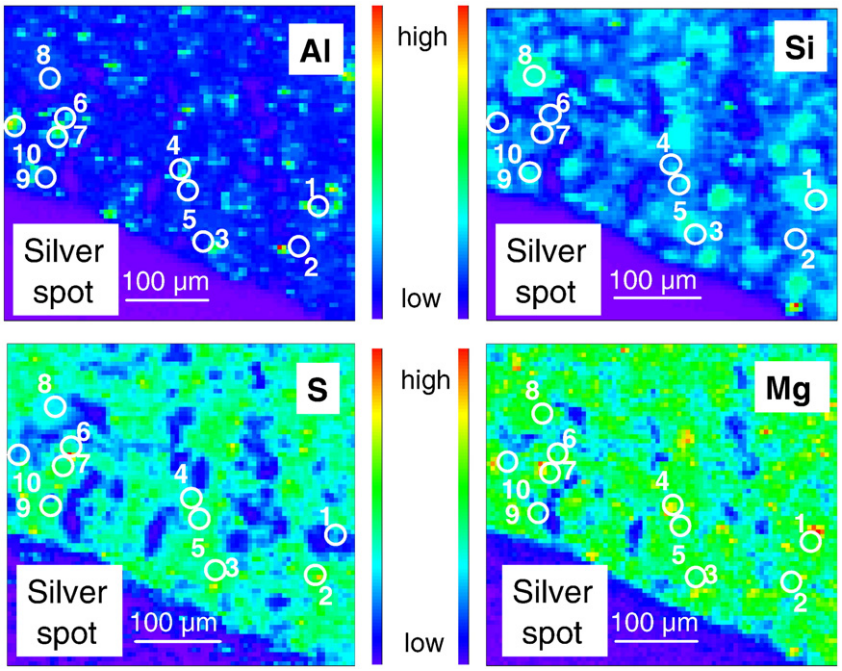

Fig. 1. Micro-XRF elemental distribution maps of Al, Si, S, and Mg in intact HCP hydrated at 50 °C. Micro-XAS selected regions for S K-edge XANES measurements are marked with numbers. A silver spot was used as marker, which appears blue on the micro-XRF maps.

appear in the spectra of ettringite and calcium monosulfoaluminate. They were previously observed both in the S K-edge XANES spectra of gypsum [15] and anhydrite [7], revealing structural similarity of these compounds. The S K-edge XANES spectra of ettringite and calcium monosulfoaluminate were found to be almost identical. Nevertheless, small differences were noticed, in particular the maximum of the oscillation in the energy range between 2490 eV and 2510 eV was slightly shifted to higher energy in ettringite compared to calcium monosulphoaluminate. Furthermore, the shape of this oscillation was smoother in the case of ettringite. The small differences in the XANES spectra have allowed ettringite and calcium monosulfoaluminate to be identified in intact cement matrices [7].

Comparison of the Al K-edge XANES spectra of the Al-bearing cement minerals revealed that the energy positions of the absorption edge of the clinker minerals (C_3A and C_4AF) and the Al-bearing cement minerals of the hydrate assemblage were shifted towards lower energy (~0.5–4 eV) compared to that of hydrotalcite (Fig. 4). This shift of the peak maximum to lower energies can be explained by changes in the symmetry of the crystal structure and/or differences in the nearest neighboring atoms [36]. Feature 'D' in the XANES spectrum of C_4AF at about 1565 eV could further indicate presence of four-fold Al [36]. The edge position of hydrotalcite could be verified based on previous measurements reported by Doyle et al. [20]. Energy position and intensity of the absorption edge in the spectrum of hydrotalcite indicate presence of six-fold Al in a dioctahedral layer [20,36–39]. The XANES spectrum of hydrotalcite consists of a broad peak (~8 eV) where two main features can be distinguished, the first one ('E' in Fig. 4) located at about 1567 eV and the second one ('F' in Fig. 4), which is very broad and intense at about 1572 eV. The spectrum of hydrotalcite is similar to that of gibbsite [39]. The latter spectrum is affected by the local symmetry. Gibbsite consists of octahedral layers with two Al sites located in distorted octahedra. A weak shoulder at about 1568 eV ('E') was further observed in the spectrum of siliceous hydrogarnet. This indicates a local symmetry similar to that of gibbsite, presumably due to distortion of the octahedral coordination. The broad and characteristic oscillation 'F' observed in all spectra in the energy range between about 1580 eV and 1590 eV could be attributed to resonances from the first coordination sphere [36]. The shape of this oscillation was found to be characteristic in the different reference spectra. Overall, the Al K-edge XANES allowed the Al-bearing cement minerals to be distinguished from each other with the exception of calcium monosulfoaluminate, calcium monocarboaluminate and tetra-calcium aluminate hydrate. The XANES spectra of these AFm-type compounds were nearly identical, suggesting that the coordination environment of Al is very similar in all AFm structures. Therefore, these compounds will be treated as a class

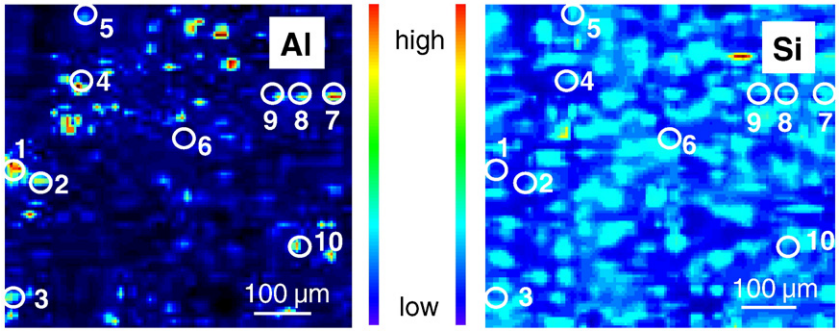

Fig. 2. Micro-XRF elemental distribution maps of Al and S in intact HCP hydrated at 50 °C. Micro-XAS selected regions for Al K-edge measurements are marked with numbers.

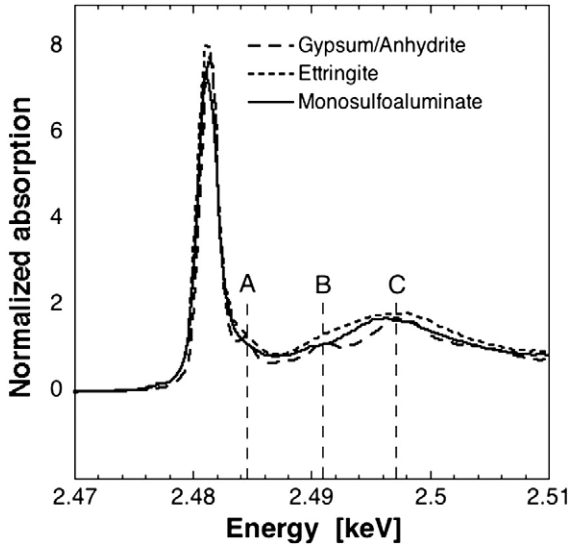

Fig. 3. S K-edge micro-XANES experimental spectrum of calcium sulfate, ettringite and calcium monosulfoaluminate. The broken lines labeled 'A', 'B' and 'C', indicate spectral features explained in the text.

of minerals rather than individual species in the following analysis of the composed XANES spectra.

3.3. Identification of cement minerals in HCP

Data analysis of the Al and S K-edge micro-XANES spectra obtained in the different ROIs was based on the assumption that several S- and Al-bearing species are present in the volume probed by the micro-focused X-ray beam (~40–80 μm^3), thus giving rise to an averaged XANES signal. Previous studies showed that a combination of PCA and TT allows the chemical species present in complex natural systems to be identified [e.g. 30,32,40]. The following procedure enabled us to decompose the averaged Al and S K-edge micro-XANES spectra into the contributions from single cement minerals.

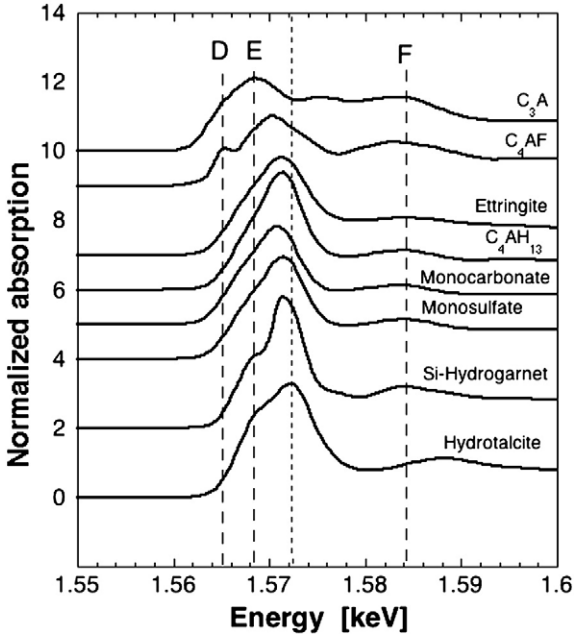

Fig. 4. Al K-edge micro-XANES experimental spectra of important Al-bearing cement minerals: aluminate (C_3A), ferrite (C_4AF), ettringite, tetra-calcium aluminate hydrate (C_4AH_{13}), calcium monocarboaluminate, calcium monosulfoaluminate, siliceous hydrogarnet and hydrotalcite. The broken lines labeled 'D', 'E' and 'F', indicate spectral features (see text). The unlabeled, dashed line serves to guide the eye, indicating the "white" line of hydrotalcite.

Gypsum or anhydrite, respectively, ettringite and calcium monosulfoaluminate are known to be the main S-bearing cement minerals in HCP [e.g., 41]. Sulfate binding to other cement minerals, such C–S–H phases, was neglected and assumed that their contribution to the mixed spectra was below the detection limit of XANES. The Al-bearing reference compounds used in this study, i.e., alite, ferrite, ettringite, AFm phases (tetra-calcium aluminate hydrate, calcium monosulfoaluminate and calcium monocarboaluminate), siliceous hydrogarnet and hydrotalcite constitute the main Al species in cement [e.g., 41,42]. Other potential Al sinks, such as Fe/Al-ettringite solid solutions, hydrogarnet or Al-bearing C–S–H phases, were considered to be quantitatively less important in the Portland cement studied and their contribution to the composed micro-XANES spectra was ignored. Principal component analysis was not applied in the analysis of S K-edge XANES spectra as three reference compounds account for a reasonable number of model components. However, PCA was applied to determine the number of components contained in the Al K-edge XANES spectra. Three components were found to be sufficient to reproduce all experimental Al K-edge spectra. Target transformation further revealed that most reference compounds could make up the principal components (SPOIL value $\leq$4.5). This value ranged between 1.6 and 2.5 for C_3A, ettringite, AFm phases and siliceous hydrogarnet. Fair agreement was predicted for C_4AF, which was expected to be a potentially important Al species in the Al-rich ROIs of the cement matrix. As previously indicated by Manceau et al. [32] PCA cannot identify a common species as a separate component if the set of ROIs contain the same fraction of this species since the method is only sensitive to variations among the sample spectra. Furthermore, it was observed that no conclusive information could be gained from PCA if the reference spectra are similar [7]. Thus, these shortcomings could explain why TT did not allow unambiguous identification of those Al-bearing cement minerals that could contribute to the composed XANES spectra.

In the subsequent step least-squares fitting was carried out using the LC tool implemented in ATHENA. Analysis of the S speciation was performed using the S K-edge reference spectra of the main S-bearing phases of the hydrate assemblage, i.e. ettringite and calcium monosulfoaluminate (Fig. 5). Gypsum or anhydrite, respectively, is expected to be thermodynamically unstable under the given conditions [18]. In general, good agreement between fit results and experimental spectra was observed, indicating that the proposed approach holds (Table 1). Either calcium monosulfoaluminate or ettringite were detected while co-existence of significant amounts of these minerals was only observed in two ROIs. This finding agrees with results from previous modelling and experimental studies on the same HCP material [17,18], suggesting that calcium monosulfoaluminate and small amounts of ettringite should be present in SRPC at hydration temperatures above 50 °C. Furthermore, the distribution of the two S-bearing cement minerals in the cement matrix is not homogeneous as ROIs containing predominantly one of these species were detected. Finally, we tested whether or not the quality of fits with *R* factors 0.01 to 0.02 could be improved by including calcium sulfate as potential reference compound. The quality of some fits could be slightly improved using all three S-bearing reference compounds, and LC fitting suggested presence of gypsum or anhydrite, respectively, in the ROIs dominated by calcium monosulfoaluminate.

The Al speciation in HCP was determined by considering three components in the LC fitting in accordance with the results from PCA. Nevertheless, it was assumed that all reference compounds could contribute to the composed XANES spectra due to lack of unambiguous information on the relevant cement minerals. In general, good agreement between fit results and experimental spectra was observed (Fig. 6). The clinker minerals were the dominant Al species in most Al-rich ROIs in accordance with the expectation from thermodynamic

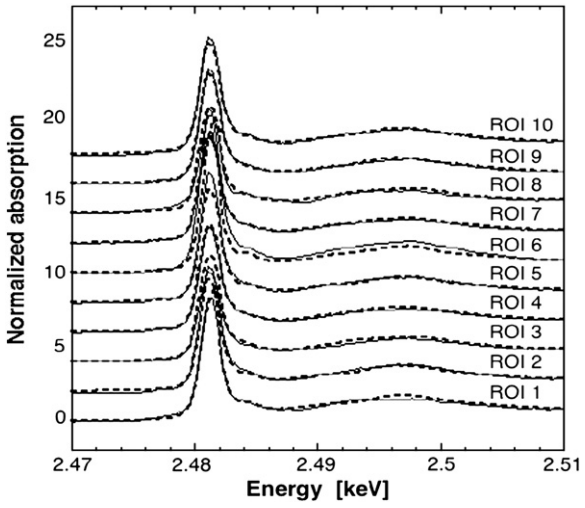

Fig. 5. S K-edge micro-XANES experimental spectra collected in ten ROIs of the intact HCP (ROIs indicated in Fig. 1). Solid lines: Experimental XANES spectra; broken lines: modeled spectra based on LC fitting.

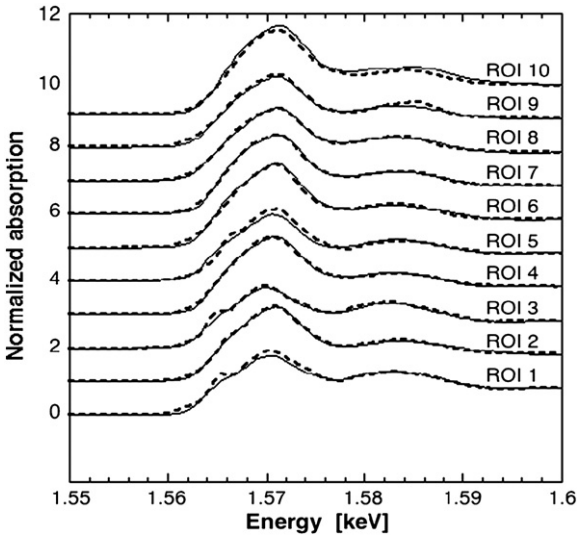

Fig. 6. Al K-edge micro-XANES experimental spectra collected in ten ROIs of the intact HCP (ROIs indicated in Fig. 2). Solid lines: Experimental XANES spectra; broken lines: modeled spectra based on LC fitting.

modelling that unreacted C_3A and C_4AF existed in the cement matrix after 28 days reaction time (Table 2) [18]. Ettringite and the AFm phases were found to be the most abundant secondary phases in the reactive zones around C_3A and C_4AF. Thus, AFm phases seem to preferentially form during hydration of SRPC at 50 °C. Interestingly, presence of hydrotalcite was indicated in some ROIs, and ettringite and hydrotalcite appeared to be minor phases forming in some reactive zones around clinker minerals. Furthermore, the Al K-edge XANES indicated that the AFm and the ettringite phases were present in spatially different reactive zones within the cement paste.

The fit parameters listed in Tables 1 and 2 correspond to relative fractions of the respective normalized reference spectra required to yield a good match between the modeled and experimental XANES spectra. Thus, while semi-quantitative phase characterization is feasible using micro-spectroscopy, quantitative analysis would require conversion of the XANES fit percentages into the more commonly used weight percentages. This would further require XANES measurements to be carried out on binary mixtures involving the reference compound of interest and the matrix. The latter approach was previously established in quantitative phase analysis from X-ray diffraction data [43] and was applied to Mn K-edge XANES data collected in transmission mode by Ressler et al. [30]. Such measurements account for the matrix-specific relationship between the intensity of the contribution of the emitted signal from a specific compound and the portion of this compound in the mixture. It is anticipated that self-absorption effects influence Al and S K-edge XANES measurements carried out in fluorescence mode, which may limit quantitative determination of phase compositions in cement matrices.

Table 1
Portions of cement minerals determined from the least-squares fitting of the S K-edge XANES spectra (ROIs 1–10 as indicated in Fig. 1). LC fits using two (normal) or three S species (italic), respectively, were taken into account for the spectra recorded in ROIs 1, 2, 5 and 6.

ROI	Calcium sulfate	Ettringite	Monosulfate	*R*-factor
1	–	–	1	0.010
	0.62 ± 0.06	–	*0.38 ± 0.06*	0.007
2	–	–	1	0.009
	0.56 ± 0.07	–	*0.44 ± 0.07*	0.007
3	–	1	–	0.021
4	–	0.59 ± 0.11	0.41 ± 0.11	0.004
5	–	–	1	0.011
	0.77 ± 0.06	–	*0.23 ± 0.06*	0.006
6	–	–	1	0.016
	0.68 ± 0.07	–	*0.32 ± 0.07*	0.009
7	–	0.99 ± 0.10	0.01 ± 0.10	0.002
8	–	1	–	0.018
9	–	0.21 ± 0.07	0.79 ± 0.10	0.002
10	–	–	1	0.002

4. Summary and conclusions

This study shows that synchrotron-based micro-XRF and micro-XANES is capable of providing information on the Al and S speciation in HCP with micro-scale resolution. X-ray fluorescence maps revealing heterogeneous Al and S distribution in the cement matrix allowed target spots (ROIs) to be identified for detailed XANES investigations. Aluminium and S K-edge XANES spectra of Al- and S-bearing single cement minerals provided the indispensable set of data required to quantify the phase composition in intact HCP material. The mineral composition was obtained from a systematic analysis of the composed Al and S K-edge XANES spectra involving PCA and TT in combination with least-squares fitting. The S K-edge XANES data reveal that calcium monosulfoaluminate and ettringite were mostly present in spatially separate ROIs of the cement matrix while they were found to co-exist only in two ROIs. The above findings substantiate results from previous modelling and experimental studies on the same HCP material, suggesting that calcium monosulfoaluminate should predominantly form at 50 °C and that the portion of ettringite should be small. The Al K-edge data shows that ettringite and AFm phases formed in Al-rich regions where the Al

Table 2
Portions of cement minerals determined from the least-squares fitting of the Al K-edge XANES spectra (ROIs 1–10 as indicated in Fig. 2).

ROI	C_3A	C_4AF	Ettringite	AFm	Hydrotalcite	*R*-factor
1	0.16 ± 0.02	0.84 ± 0.02	–	–	–	0.003
2	0.22 ± 0.02	0.34 ± 0.02	0.44 ± 0.03	–	–	0.001
3	0.14 ± 0.02	0.86 ± 0.02	–	–	–	0.003
4	0.36 ± 0.02	0.07 ± 0.02	0.57 ± 0.03	–	–	0.002
5	0.13 ± 0.01	0.48 ± 0.02	–	0.39 ± 0.02	–	0.001
6	0.50 ± 0.01	–	–	0.32 ± 0.03	0.18 ± 0.03	0.002
7	0.41 ± 0.01	–	–	0.47 ± 0.02	0.12 ± 0.02	0.001
8	0.31 ± 0.01	0.42 ± 0.02	–	0.27 ± 0.02	–	0.001
9	0.20 ± 0.01	0.45 ± 0.02	–	0.35 ± 0.02	–	0.001
10	0.48 ± 0.01	–	–	0.33 ± 0.03	0.19 ± 0.04	0.003

speciation was dominated by the presence of the clinker minerals aluminate and ferrite. Ettringite and the AFm phases were observed in spatially separate ROIs of the cement matrix, which agrees with the results from S speciation. In addition, hydrotalcite was detected as newly forming phase in a few reactive zones of the cement matrix.

Acknowledgments

The authors wish to thank Dr. T. Matschei (Empa/Aberdeen), K. Rozov (PSI) and L. Aimoz (PSI) for synthesis and supply of reference compounds. Thanks are extended to D. Kunz (PSI) for sample preparation and assistance during the measuring campaigns. T. Beckmann (Soil morphology, Schwülper-Lagersbüttel) is thanked for the preparation of thin sections. Dr. M. Janousch is gratefully acknowledged for technical assistance on the LUCIA beamline and the Swiss Light Source (SLS) for provision of beamtime.

Partial financial support was provided by the National Cooperative for the Disposal of Radioactive Waste (Nagra), Switzerland.

References

[1] J. Skibsted, C. Hall, Characterization of cement minerals, cements and their reaction products at the atomic and nano scale, Cement Concrete Res. 38 (2008) 205–225.
[2] C. Famy, K.L. Scrivener, A. Atkinson, A.R. Brough, Effects of an early or a late treatment on the microstructure and composition of inner C–S–H products of Portland cement mortars, Cement Concrete Res. 32 (2002) 269–278.
[3] K.L. Scrivener, Backscattered electron imaging of cementitious microstructures: understanding and quantification, Cem. Concr. Comp. 26 (2004) 935–945.
[4] I.G. Richardson, The calcium silicate hydrates, Cement Concrete Res. 38 (2008) 137–158.
[5] M. Vespa, R. Dähn, E. Gallucci, D. Grolimund, E. Wieland, A.M. Scheidegger, Micro-scale investigation of Ni uptake by cement using a combination of scanning electron microscopy and synchrotron-based techniques, Environ. Sci. Technol. 40 (2006) 7702–7709.
[6] M. Vespa, R. Dähn, D. Grolimund, E. Wieland, A.M. Scheidegger, Co speciation in hardened cement paste: a macro- and micro-spectroscopic investigation, Environ. Sci. Technol. 41 (2007) 1902–1908.
[7] M. Vespa, E. Wieland, R. Dähn, D. Grolimund, A.M. Scheidegger, Determination of the elemental distribution and chemical speciation in highly heterogeneous cementitious materials using synchrotron-based micro-spectroscopic techniques, Cement Concrete Res. 37 (2007) 1473–1482.
[8] P.J. Durham, Theory of XANES, in: D.C. Koningsberger, R. Prins (Eds.), X-ray Absorption — Principles, Applications, Techniques of EXAFS, SEXAFS, and XANES, John Wiley, New York, 1988.
[9] N. Richard, N. Lequeux, P. Boch, An X-ray absorption study of phases formed in high-alumina cements, Adv. Cem. Res. 7 (28) (1995) 159–169.
[10] N. Richard, N. Lequeux, P. Boch, Local environment of Al and Ca in CAH_{10} and C_2AH_8 by X-ray absorption spectroscopy, Eur. J. Sol. State Inor. Chem. 32 (1995) 649–662.
[11] N. Richard, N. Lequeux, P. Florian, Changes in the structure of $CaAl_2O_{14}H_20$ during heat treatments: an X-ray absorption spectroscopy and ^{27}Al NMR study, in: P. Colombet, A.R. Grimmer, H. Zanni, P. Sozanni (Eds.), Nuclear Magnetic Resonance Spectroscopy of Cement-based Materials, Springer-Verlag, Berlin, 1998.
[12] R.J. Kirkpatrick, G.E. Brown, N. Xu, X. Cong, X-ray absorption spectroscopy of C–S–H and some model compounds, Adv. Cem. Res. 9 (1997) 31–36.
[13] N. Lequeux, A. Moreau, S. Philippot, P. Boch, Extended X-ray absorption fine structure investigation of calcium silicate hydrates, J. Am. Ceram. Soc 82 (1999) 1299–1306.
[14] J. Verstraete, L. Khouchaf, D. Bulteel, E. Garcia-Diaz, A.M. Flank, M.H. Tuilier, Amorphisation mechanism of a flint aggregate during the alkali–silica reaction: X-ray diffraction and X-ray absorption XANES contributions, Cement Concrete Res. 34 (2004) 581–586.
[15] S. Pattanaik, G.P. Hoffman, S. Sahu, R.J. Lee, X-ray absorption fine structure spectroscopy and X-ray diffraction study of cementitious materials derived from coal combustion by-products, Cement Concrete Res. 34 (2004) 1243–1249.
[16] A. Roy, Sulfur speciation in granulated blast furnace slag: an X-ray absorption spectroscopic investigation, Cement Concrete Res. 39 (2009) 659–663.
[17] B. Lothenbach, F. Winnefeld, C. Alder, E. Wieland, P. Lunk, Effect of temperature on the pore solution, microstructure and hydration products of Portland cement pastes, Cement Concrete Res. 37 (2007) 483–491.
[18] B. Lothenbach, T. Matschei, G. Möschner, F.P. Glasser, Thermodynamic modelling of the effect of temperature on the hydration and porosity of Portland cement, Cement Concrete Res. 38 (2008) 1–18.
[19] B. Lothenbach, E. Wieland, A thermodynamic approach to the hydration of sulphate-resisting Portland cement, Waste Manag. 26 (2006) 706–719.
[20] C.S. Doyle, S.J. Traina, H. Ruppert, T. Kendelewicz, J.J. Rehr, G.E. Brown, XANES studies at the Al K-edge of aluminium-rich surface phases in the soil environment, J. Synchrotron Radiat. 6 (1999) 621–623.
[21] M. Atkins, D. Macphee, A. Kindness, F.P. Glasser, Solubility properties of ternary and quaternary compounds in the $CaO–Al_2O_3–SO_3–H_2O$ system, Cement Concrete Res. 21 (1991) 991–998.
[22] T. Matschei, B. Lothenbach, F.P. Glasser, The AFm-phase in Portland cement, Cement Concrete Res. 37 (2007) 118–130.
[23] T. Matschei, Thermodynamics of cement hydration, Thesis, University of Aberdeen, 2007.
[24] K. Rozov, U. Berner, C. Taviot-Gueho, D. Kulik, F. Leroux, G. Renaudin, Synthesis and characterization of LDH hydrotalcite–pyroaurite solid solution series, Cem. Concr. Res. (in press).
[25] A.M. Flank, C. Cauchon, P. Lagarde, S. Bac, M. Janousch, R. Wetter, J.M. Dubuisson, M. Idir, F. Langlois, T. Moreno, D. Vantelon, LUCIA, a microfocus soft XAS beamline, Nucl. Instrum. Methods Phys. Res. B 246 (2006) 269–274.
[26] M. Marcus, A.A. MacDowell, R. Celestre, A. Manceau, T. Miller, H.A. Padmore, R.E. Sublett, Beamline 10.3.2 at ALS: a hard X-ray microprobe for environmental and material sciences, J. Synchrotron Radiat. 11 (2004) 239–247.
[27] M. Neville, IFEFFIT: interactive EXAFS analysis and FEFF fitting, J. Synchrotron Radiat. 8 (2005) 322–324.
[28] B. Ravel, M. Neville, ATHENA, ARTEMIS, HEPHAESTUS: data analysis for X-ray absorption spectroscopy using IFEFFIT, J. Synchrotron Radiat. 12 (2005) 537–541.
[29] L. Tröger, D. Arvanitis, K. Baberschike, H. Michaelis, U. Grimm, E. Zschech, Full correction of the self-absorption effect in soft-fluorescence extended X-ray absorption fine structure, Phys. Rev. B 46 (1992) 3283–3289.
[30] T. Ressler, J. Wong, J. Roos, I.L. Smith, Quantitative speciation of Mn-bearing particulates emitted from autos burning (methylcyclopentadienyl) manganese tricarbonyl-added gasoline using XANES spectroscopy, Environ. Sci. Technol. 34 (2000) 950–958.
[31] E.R. Malinowski, Factor Analysis in Chemistry, 2nd ed. John Wiley, New York, 1991.
[32] A. Manceau, M.A. Marcus, N. Tamura, Quantitative speciation of heavy metals in soils and sediments by synchrotron X-ray techniques, in: P.A. Fenter, M.L. Rivers, N.C. Sturchio, S.R. Sutton (Eds.), Application of Synchrotron Radiation in Low-Temperature Geochemistry and Environmental Science, Mineralogical Society of America, Washington, DC, 2002.
[33] D. Li, G.M. Bancroft, M. Kasrai, M.E. Fleet, X. Feng, K.H. Tan, S K- and L-edge X-ray absorption spectroscopy of metal sulfides and sulfates: applications in mineralogy and geochemistry, Can. Mineral. 33 (1995) 949–960.
[34] E. Paris, G. Giuli, M.R. Caroll, The valence and speciation of sulfur in glasses by X-ray absorption spectroscopy, Can. Mineral. 39 (2001) 331–339.
[35] M. Fleet, X. Liu, S.L. Harmer, P.L. King, Sulfur K-edge XANES spectroscopy: chemical state and content of sulfur in silicate glasses, Can. Mineral. 43 (2005) 1605–1618.
[36] P. Ildefonse, D. Cabaret, P. Sainctavit, G. Calas, A.-M. Flank, P. Lagarde, Aluminium X-ray absorption near edge structure in model compounds and earth's surface minerals, Phys. Chem. Miner. 25 (1998) 112–121.
[37] D.A. McKeown, G.A. Waychunas, G.E. Brown, EXAFS study of the coordination environment of aluminium in a series of silica-rich glasses and selected minerals within the $Na_2O–Al_2O_3–SiO_2$ systems, J. Non-Cryst. Solids 74 (1985) 349–371.
[38] D. Li, M. Bancroft, M.E. Fleet, X.H. Feng, Y. Pan, Al–K edge XANES spectra of aluminosilicate, Am. Mineral. 80 (1995) 432–440.
[39] A. Mottana, J.L. Roberts, A. Marcelli, G. Giuli, G. Della Ventura, E. Paris, Z. Wu, Octahedral vs. tetrahedral Al coordination in synthetic micas by XANES spectroscopy, Am. Mineral. 82 (1997) 497–502.
[40] A. Voegelin, S. Pfister, A.C. Scheinost, M. Marcus, R. Kretzschmar, Changes in zinc speciation in field soil after contamination with zinc oxide, Environ. Sci. Technol. 39 (2005) 6616–6623.
[41] H.F.W. Taylor, Cement Chemistry, 2nd ed., Thomas Telford, London, 1997.
[42] B. Lothenbach, F. Winnefeld, Thermodynamic modeling of the hydration of Portland cement, Cement Concrete Res. 36 (2006) 209–226.
[43] H.P. Klug, L.E. Alexander, X-ray Diffraction Procedures for Polycrystalline and Amorphous Materials, 2nd ed., John Wiley, New York, 1974.